CROATICA CHEMICA ACTA CCACAA 63 (3) 417—432 (1990)

CCA-1948

YU ISSN 0011-1643
UDC 541.183
*Conference Paper (Invited)*

# Pyrite Photoanode/Redox Electrolyte Interface: Characterization of the Interaction of the Reducing Species with Pyrite Through Temperature Dependence Measurements*

*Nicolás Alonso-Vante and Helmut Tributsch*

*Hahn-Meitner-Institut, Abt. Solare Energetik, Glienicker Straße 100 D-1000 Berlin 39, F. R. G.*

Received May 4, 1990

At the semiconductor pyrite photoanode/electrolyte interface, the interaction of the reducing species containing-electrolyte was investigated by temperature dependence measurements. An increase of negative entropy turnover could be related to negatively charged species interacting with the positively charged pyrite surface. Further studies, using the impedance technique in darkness and under illumination, showed that kinetic and diffusion-like processes control this interface. In the determination of the activation energy both dc and ac techniques lead to compatible results.

## INTRODUCTION

Pyrite represents an interesting model system for solar energy materials among the sulfide semiconducting materials. Firstly because it is very abundant in nature[1] and secondly, due to its property of absorbing visible light within approx. 200 Å ($\alpha > 6.0 \cdot 10^5$ cm$^{-1}$ for $h\nu > 1.3$ eV)[2]. This latter suggests that it might be possible to use this material in the form of thin photoactive films. Previous investigations using pyrite in polycrystalline and single crystal form pointed towards a complex interfacial behaviour in photoelectrochemical cells. Previous electrochemical studies diverge in the interpretation of the pyrite interfacial reactions.[3,4] These discrepancies are probably due to the different stoichiometry inherent to the material as reported recently by our group for synthetic pyrite.[5]

It was demonstrated by the RRDE technique, that the pyrite ($FeS_2$) photoanode reaches a stabilization factor approaching 100% when using reducing agents, *e. g.*, $I^-$, $Br^-$ in sufficiently high concentration.[6] Positive ions ($Fe^{2+}$, $Mn^{2+}$) or complexes ($Fe(phen)_3^{2+}$), in comparable concentrations, cannot induce such

---

* Based on an invited lecture presented at the *8th »Ruđer Bošković« Institute's International Summer Conference on the Chemistry of Solid/Liquid Interfaces* Red Island, Rovinj, Croatia, Yugoslavia, June 22 — July 1, 1989.

efficient stabilization. However, addition of $Cl^-$ to a solution containing $Fe(phen)_3^{2+}$ improves electron transfer. This was explained in terms of a coordination chemistry mediated by $Cl^-$ ions with the pyrite semiconductor surface.[7]

Taking into account the above mentioned complications, we have focussed our attention in investigating how different reducing species interact with the pyrite interface by means of a temperature variation.

## EXPERIMENTAL

Single crystals of pyrite were synthesized from its elements by the chemical vapor transport (CVT) method.[8] Back-ohmic contacts were made with euthetic In-Ga amalgam. The crystals were fixed with silver paste (Scotchcast 3M) onto brass shafts of Vespel holders and insulating epoxy resin (Scotchcast 3M) was used to encapsulate the crystals. The exposed electrode surfaces were mechanically polished to a mirror finish with diamond paste (Winter corp., down to 0.25 μm) and rinsed with bidistilled water. A standard photoelectrochemical apparatus was used for the recordings of (photo)current-voltage curves. Illumination was supplied by a halogen-W lamp (250 W). The cell was provided with a double wall for the temperature control bath in which the working and the counter electrode were placed. The reference electrode ($Hg_2SO_4$) compartment was a unit apart and connected to the cell through a bridge with a Luggin capillary. The reference electrode was maintained at room temperature. The impedance data were obtained by a computer-aided system (EGG potentiostat Mod 273, Two phase Lock-in and a HP computer Mod. 93000) with a software developed in this laboratory. The amplitude of the ac signal was typical 2 mV (rms).

## RESULTS AND DISCUSSIONS

### *Cyclic Voltammograms*

Due to the complex nature of the pyrite surface, we proceeded to obtain the electrochemical fingerprint of our synthetic single crystal after it was left in air, etched, and after hydrogen evolution in 0.5 M $HClO_4$ in order to have a better control and reproducibility of it before any photoelectrochemical experiment was undertaken. In the range of the scanned potential (after stabilization between 5 to 10 minutes) two surface reactions were identified at —0.56 and —0.39 V/$Hg_2SO_4$, respectively. Figure 1 summarizes the typical behaviour of the pyrite semiconducting electrode in this medium. The observed peak current intensity of the voltammetric curves actually depends on the treatment followed. For the sake of comparison, we have chosen hydrogen evolution (passed charge approximately 4 C/cm² at —1.25 V/$Hg_2SO_4$) since we know that this treatment enhances the photoresponse of the pyrite/redox species interface.[9] The curve depicted in Figure 1C represents this characteristic, in which the current intesity peaks corresponding to the formal surface redox potential of —0.39 V/$Hg_2SO_4$ are enhanced in comparison to those represented on the curves A and B. As a result, the intensity of these current peaks are alterated depending upon whether the pyrite surface is subjected to a process of electrochemical reduction or to oxidation in acid medium. This effect, *a prori*, evidences that the observed surface reactions are not interrelated and of different nature. It is believed that during the oxidation process, in acid medium, the predominant reaction is:

$$FeS_2 + 8H_2O \rightarrow Fe^{3+} + 2SO_4^{2-} + 16H^+ + 15e^- \quad (1)$$

whereas with a cathodic polarization the pyrite reacts according to:

$$FeS_2 + 4H^+ + 4e^- \rightarrow Fe^0 + H_2S \quad (2)$$

with a subsequent oxidation step

$$Fe^0 \rightarrow Fe^{2+} + 2e^- \quad (3)$$

Without going into the mechanistic details as discussed by others,[4] and according to our measurements performed on synthetic as well as natural samples, we arrive at the conclusion that reaction (1) leads to the formation of an hydrated iron oxide. This latter appears to be associated with the electrochemical response at —0.56 V/$Hg_2SO_4$, (Figure 1) which increases with increasing oxidation of the pyrite sample. X-ray photoelectron spectroscopy (XPS) performed on the electrochemically oxidized or air oxidized surface[10,11] has indeed revealed the presence of iron oxide without discerning its chemical composition. Moreover, the effect of the proton reduction at the pyrite interface produces hydrogen disulfide evolution which not only modifies the morphology of the exposed crystalline oriented surface but also enhances the photoactivity of the crystals. This would mean that during this process a loading of hydrogen into the pyrite lattice may occur, reducing in this way defects or recombination centers on the surface and within the space charge layer as discussed by us[9] and by other authors[12] using other materials. A parallel increase of the surface roughness has been observed. Since hydrogen is expected to react with sulfur species (*e. g.*, FeS) a change in the oxidation state may occur with one of the sulfur compounds involved. Spectroscopic studies will be needed to identify the species.

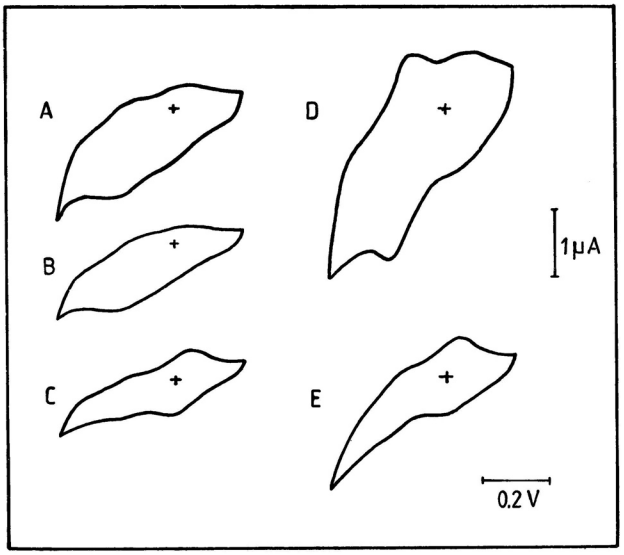


Figure 1. Stabilized cyclic voltammograms for differently treated pyrite surfaces in 0.5 M $HClO_4$, at a scan rate of 150 mV/s. (A) after polishing with diamond past; (B) after etching in a HF:$CH_3COOH$:$HNO_3$ (1:1:2) solution; (C) after hydrogen evolution; (D) and (E) after photoelectrochemical measurements reaching and avoiding the oxidation potential of the pyrite surface, respectively. The cross point is placed at —0.4 V with respect to the $Hg_2SO_4$ reference electrode. Electrode surface area is 0.037 $cm^2$.

As observed in the voltammograms of Figure 1, there is not complete disappearance of the more negative surface reaction attributed to the iron oxide. From these experiments it is concluded that a small amount of oxide (in monolayer quantity) is always present at the hydrogen activated surface.

*Entropy Change due to the Effect of Light*

The photopotential of the pyrite/redox electrolyte interface as a function of temperature is shown in Figure 2. The slopes of the lines for the systems containing $I^-$, $[Fe(CN)_6]^{4-}$, Mohr's salt and $Fe(ClO_4)_2$ upto 45 °C are all roughly the same. For the system containing $FeSO_4$ the slope differs by 40% (Figure 2A). The characteristic of this set of experiments is that the photo-

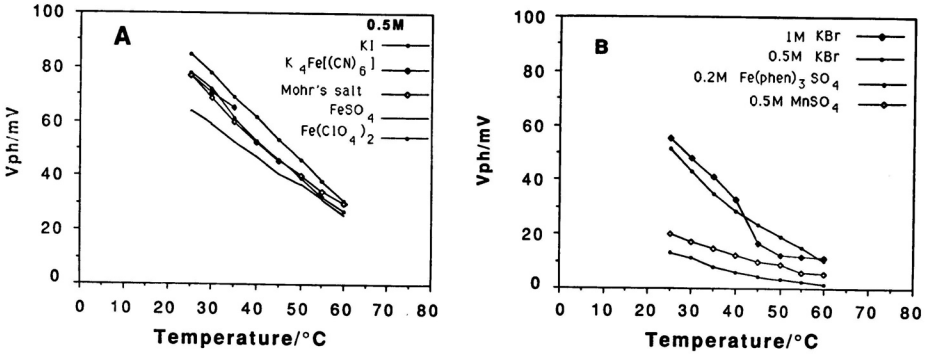


Figure 2. Variation of the photopotential as a function of temperature for different systems. Plots A and B summarize those systems which are characterized by curve (E) and by curve (D) (from Figure 1), respectively. For the photoelectrochemical measurements the base electrolyte was 0.5 M $H_2SO_4$. With $Fe(ClO_4)_2$, 0,5 M $HClO_4$ was used. For the determination of the slope $(\partial V_{ph}/\partial T)$ in B, only the first 5 points were considered.

potential as a function of temperature is reversible when cooling down to 25 °C. This behaviour is understandable since the redox potential of the corresponding species remain negative from the oxidation potential of the pyrite electrode. Moreover, for the systems containing KBr, $Fe(phen)_3SO_4$ and $MnSO_4$, the redox potentials of which are more positive than the pyrite oxidation potential, the slope changes at *ca.* 40 °C. The increase of the temperature in combination or suitable oxidation potential, at the interface, may be the reason for these systems not being reversible (iron oxide formation) when cooling down 25 °C. This expectation is again confirmed in recording afterwards the cyclic voltammograms in which the surface reaction at —0.56 V/$Hg_2SO_4$ is enhanced, (see Figure 1D). In the range of reversibility, *i. e.*, from 25 °C upto 40 °C, the variation of the photopotential with temperature $(\partial V_{ph}/\partial T)$ is to a first approximation a measure, in equilibrium conditions, of the entropy change. This change can be related to the degree of strong or weak interaction of the species with the semiconductor surface. By subtracting the entropy change due to a solvation effect ($\Delta S_{sol}$) of the same species in the electrolyte (by measuring the equilibrium potential at a platinum electrode as a function of temperature), we were then able to get the entropy change due to the effect of light, $\Delta S_{ph}$, according to the equation:

$$\Delta S_{ph} = (nF)^{-1} (\partial V_{ph}/\partial T) - \Delta S_{sol} \quad (4)$$

The strong interaction of a redox species may imply an increase of the negative entropy change. This phenomenon is in principle favoured when the positively charged pyrite surface interacts with species possessing a negative charge. It was then interesting to investigate and compare how efficient this interaction is with complexes containing differently coordinated iron. In order to visualize this effect we have plotted the photocurrent generated (in log scale) at the oxidation half-wave potential of the corresponding species corrected for the same light intensity as a function of the entropy change under light, $\Delta S_{ph}$, Figure 3. From this figure and with the help of Figure 1 we can

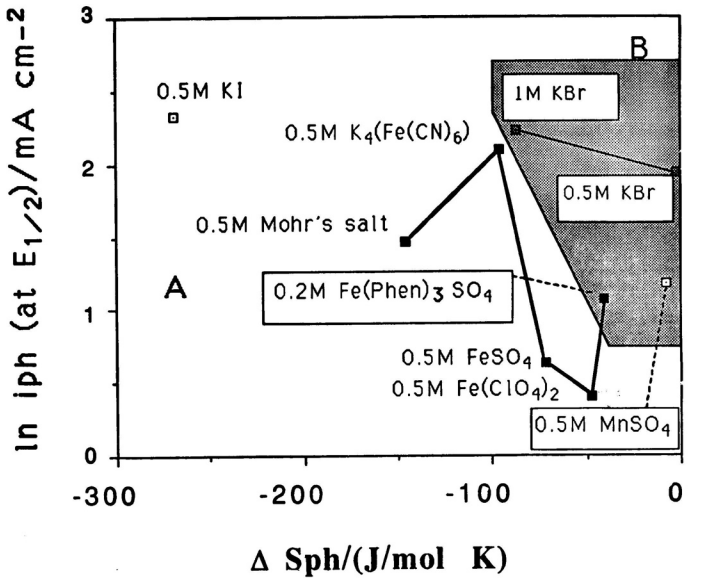


Figure 3. Photocurrent density (corrected to 40 mW/cm$^2$) at the half wave potential as a functi n of the negative entropy change for the species described in the Figure 2. Regions A and B indicate absence and presence of surface electrochemical oxidation of pyrite, respectively.

recognize two regions: in the region marked A an additional electrochemical oxidation of the semiconductor surface is avoided. Here negatively charged species, which can chemically interact with the electrode surface (*e. g.*, $I^-$), and complexes which can interact with the electrode surface *via* their ligand shells are characterized by high photocurrent densities and comparatively high entropy changes (*e. g.*, $[Fe(CN)_6]^{4-}$ and the Mohr's salt: $(NH_4)_2SO_4Fe(SO_4)_2$). On the other hand, positive ions as $Fe^{2+}$ in sulfate or perchlorate, respectively which cannot interact chemically with iron centers on the pyrite surface produce low photocurrent densities and low negative entropy changes. In region B the photooxidation of the species is accompained by the electrochemical oxidation of the chemical change of the electrode interface (OH- and -O- groups in the uppermost surface layer) the situation is now reversed. Negative

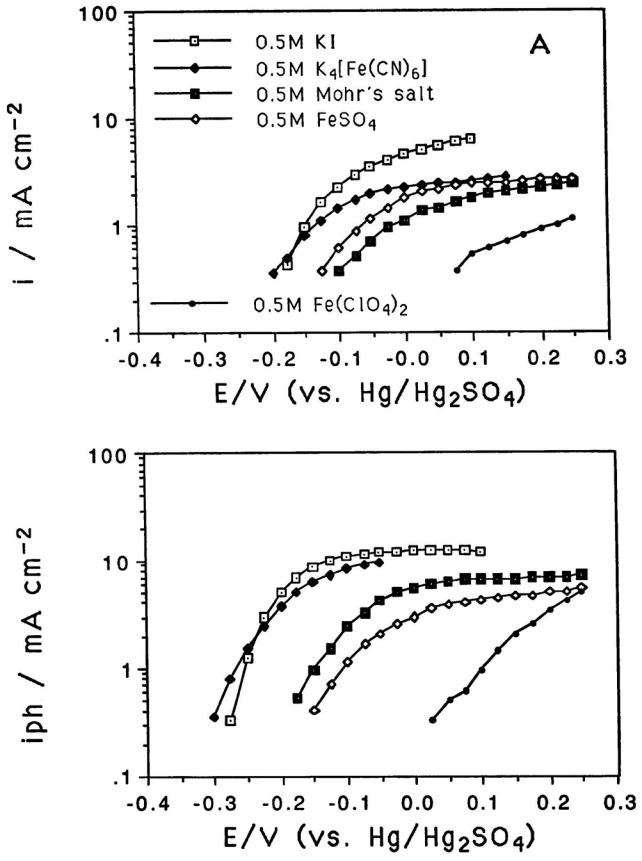


Figure 4. *Fig. 4 to be continued*

ions (Br) generate somewhat lower photocurrents while yielding considerably smaller negative entropy changes. Positively charged species appear to yield somewhat higher current densities than iron in sulfate and perchlorate with the non-oxidized surface (region A).

## *Current-potential Characteristics*

In spite of the reasonable good quality of the pyrite-photoanode interface for photoconversion purposes, the dark anodic current obtained varied as a function of the reducing agents and as a function of temperature. Following the same criterium adopted for the Figures 2 and 3, we plotted the ensemble of current-potential curves in darkness as well as under illumination for the different systems at 25 °C. Figure 4 visualized these results. As can be observed, for the systems represented in the Figure 4A, very high anodic dark current densities are obtained (where pyrite anodic corrosion is avoided). These anodic dark currents vary in decreasing order of magnitude (at 0 V); $i_{KI} > i_{K_4[Fe(CN)_6]} > i_{FeSO_4} > i_{Mohr} > i_{Fe(ClO_4)_2}$. Moreover, for the systems represented in Figure 4B (whe-

*Fig. 4 continued*

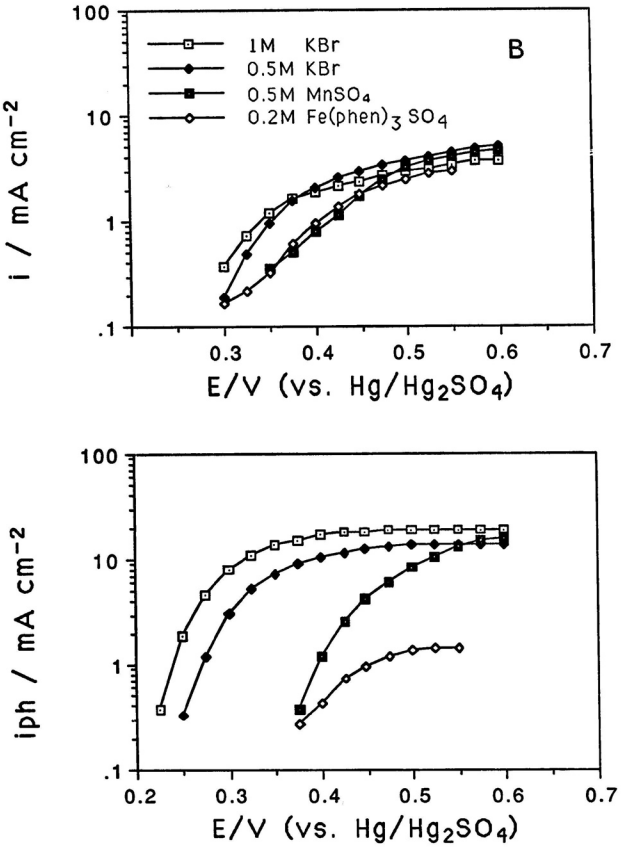


Figure 4. Current potential curves in darkness (upper) and under illumination (lower). Plots A and B summarize those systems which are characterized by curve (E) and by curve (D) (from Figure 1), respectively.

re anodic corrosion of pyrite occurs) the dark anodic current, at 0.4 V, is: $i_{KBr} > i_{Fe(phen)_3SO_4} > i_{MnSO_4}$. These dark anodic currents are caused *a priori* by the electron transfer from the electrolyte to the semiconductor bulk *via* interface states. Under illumination, almost the same trend (Figure 4A) is obtained except for the fact that $i_{(ph)Mohr}$ and $i_{(Ph)FeSO4}$ are inverted. In the case of Figure 4B the photocurrents obtained follow the same trend as in the darkness. At 0.4 V the photocurrent obtained with KBr is one order of magnitude bigger than that obtained with $MnSO_4$ and iron phenanthroline. The increase, at more positive polarization, of the photocurrent with $MnSO_4$ and iron phenanthroline indicates that a parallel reaction due the corrosion of the semiconductor is involved.[7]

The parallel trend and magnitudes of the currents in darkness as well as under illumination observed in our current-potential curves can not be explained in classical theories based on tunnel mechanism. An explanation must be

found in terms of coordinative chemistry. This implies that the charge transfer mechanism is proceeding over d-states of pyrite. Concerning the quantum yield, it is possible to deduce it from the photocurrent potential curves. As reported by our group,[10] a quantum yield $>90\%$ is obtained with the Pyrite/($I^-/I_3^-$) system. From this value and with the help of Figure 3 (region A, where pyrite corrosion does not occur) it is possible to deduce the corresponding quantum effeciencies of the other species. These values range from 15%, 24%, 56%, 80% to 90%, for $Fe(ClO_4)_2$, $FeSO_4$, $K_4[Fe(CN)]_6$, Mohr' salt and KI, respectively. This means that a proportional relation is to be found between the negative entropy change and the quantum efficiency, in other words a direct relation with the degree of interaction of the species with the pyrite semiconducting surface. Figure 5 displays for the pyrite/KI, KBr systems the current potential

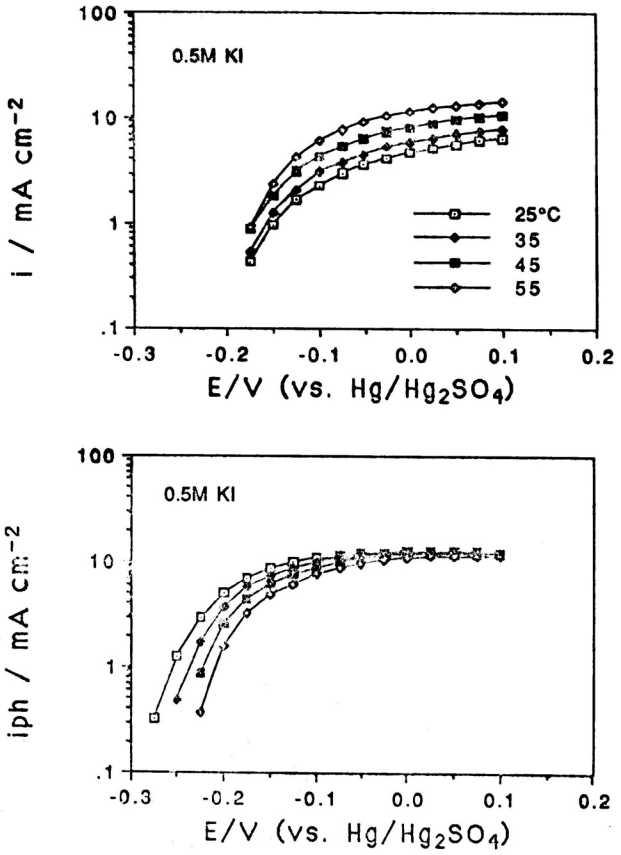


Figure 5. *Fig. 5 to be continued*

curves as a function of temperature in darkness and under illumination. As observed in both systems repressented here, in the anodic potential range, the dark currents obey classical electrochemical laws as expected from the kinetics of charge transfer in the low potential region. In the case of a semicon-

*Fig. 5. continued*

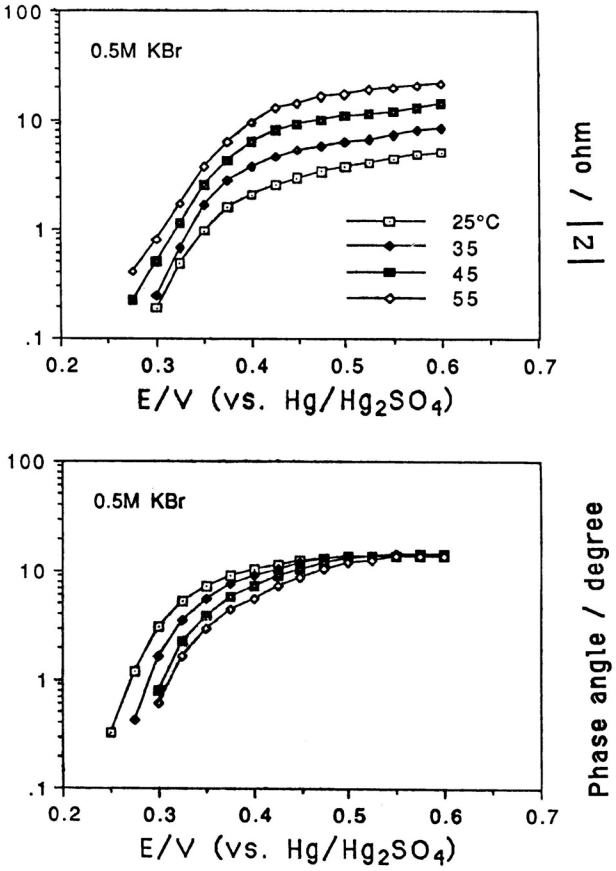


Figure 5. Current-potential curves as a function of temperature in darkness (top) and under illumination (bottom) for the system containing 0.5 M KI and 0.5 M KBr.

ductor, the fact that such a dark current increases can be due to lowering of the barrier, which means that the injection of electron by the electroactive species will be favoured by the Boltzmann factor, $\exp(-q/kT)$. On the other hand, a plateau is attained at higher potential bias, probably due to a diffusion-like effect and/or total coverage of the interacting sites of the semiconducting surface. This situation will be discussed below in the impendance section. An Arrhenius type plot (Figure 6) can be obtained for the dark current in the low potential region. The activation energy (at an overpotential of —46 mV) for these systems are: 0.26 and 0.46 eV, respectively. On the other hand, the curves under illumination show that in the low potential region the kinetics of recombination is favoured as the temperature increases. This is associated with a lowering of the photopotential already described above. At higher anodic potential bias a plateau is obtained for both systems, independent of the temperature, which means that the number of carriers produced by photons are totally separated by the high field existent in the space charge region of the semiconductor.

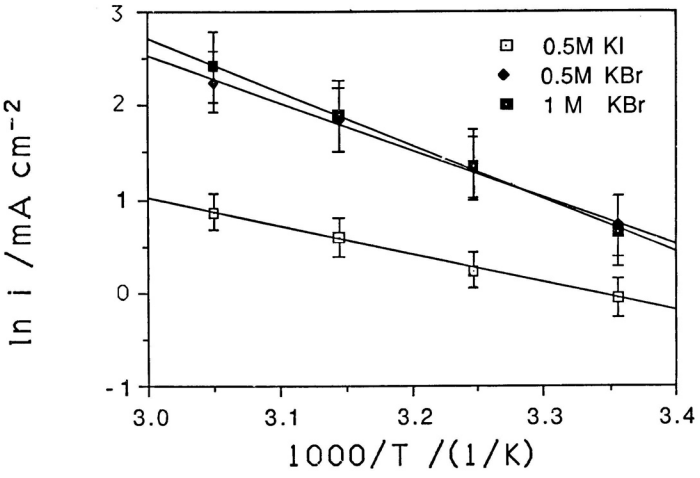


Figure 6. Arrhenius type plot deduced from measurements in Figure 5 (in darkness) at an overpotential of —46 mV, for 0.5 M KI, 0.5 M KBr and 1 M KBr.

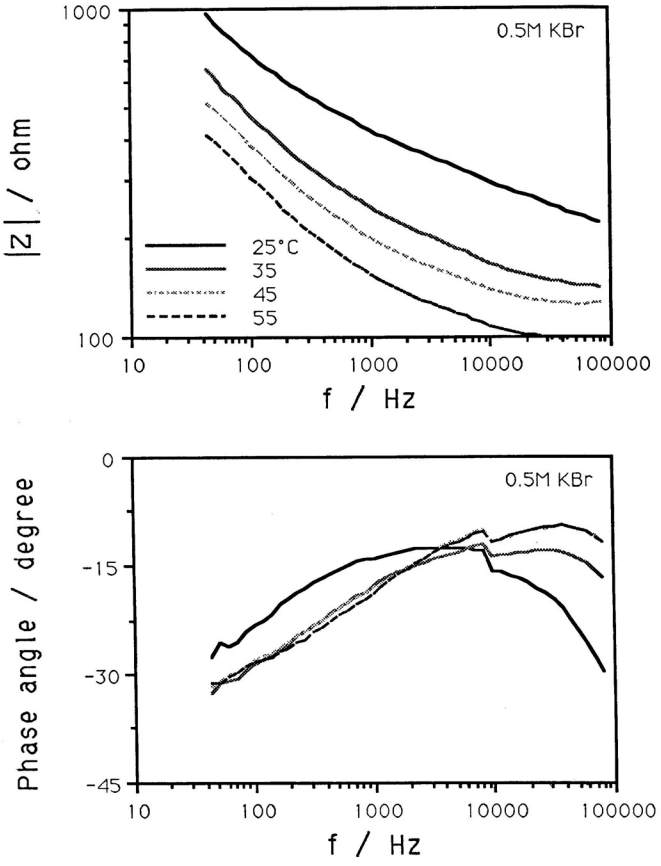


**Figure 7.** *Fig. 7 to be continued*

*Fig. 7 continued*

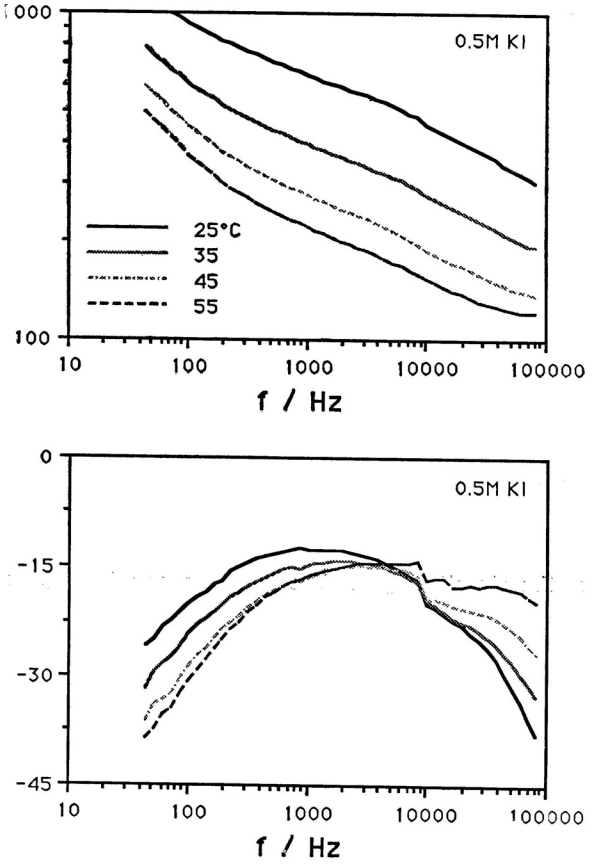


Figure 7. Bode plots (impedance magnitude and phase angle) as a function of temperature in darkness for the systems containing 0.5 M KI and 0.5 M KBr. Electrode surface area is 0.037 $cm^2$.

## *Impedance Measurements*

The impendance spectra were recorded as a function of temperature in darkness and under illumination at discrete polarization values, *i. e.*, mainly where dark and photocurrent were small. As model experiments, we have taken again the systems pyrite/KI, KBr (Figure 5). Figure 7 shows the Bode representation corrected for series resistance: log ($|Z|$) *vs.* log (frequency) and phase angle *vs. log* (frequency) plots of these systems in darkness at (—0.24 V, and 0.28 V), respectively. The decrease of the impendance modulus with temperature is readily observed in the whole frequency range. From these Bode diagrams it can be seen that at least 3 different relaxation times are present at both systems. The influence of light although interesting but more complicated will not be discussed here. The systems which we analyse now actually represent the best example in terms of photoconversion on the pyrite photoanode material. In order to identify the different components we looked

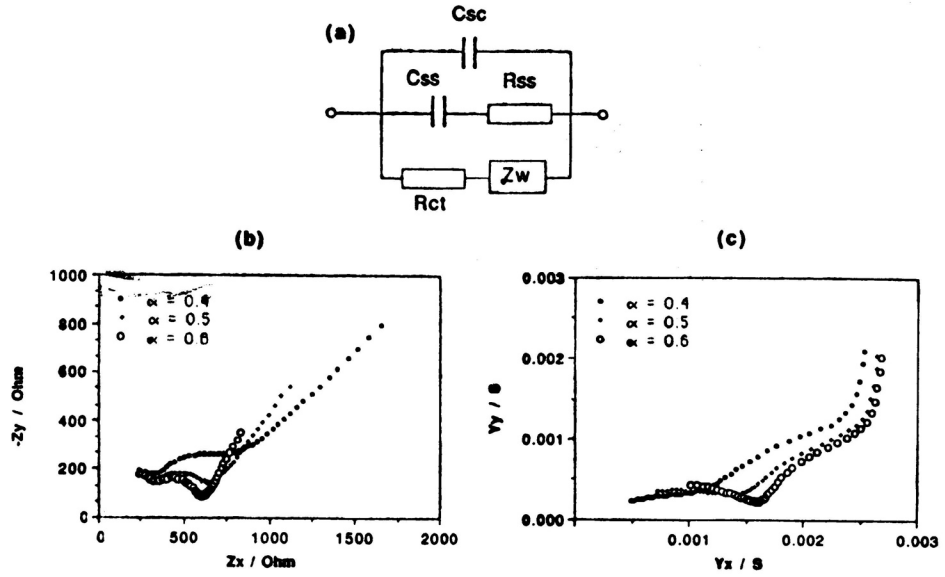


**Figure 8.** (a)shows the circuit employed to simulate our data. (b) and (c) show the corresponding impedance plane plot and the admittance plane plot of this circuit as a function of $\alpha$. The values given to the other parameters are as follows: $C_{sc}$ = 0.0036 $\mu$F, $C_{ss}$ = 0.01 $\mu$F, $R_{ss}$ = 1000 $\Omega$, $R_{ct}$ = 580 $\Omega$ and $\sigma'$ = 12700 $\Omega$/s.

for a circuit that would agree with our experimental data over the measured frequency range. The circuit which best fits our data is represented in Figure 8, which also shows the simulated impendance and admitance plots at three values of the parameter $\alpha$. $R$ and $C$ stand for resistors and capacitors, respectively. This simulation will help to judge the influence of $\alpha$ on the impendance behaviour in the following analysis, see Figure 10b. The subindexes (sc), (ss) and (ct) represent the semiconductor, the surface states and charge transfer, respectively. The box $Z_w$ stands for a »generalized« Warburg impendance which is of the form:

$$Z_w = \sigma' (i\omega)^{-\alpha} \tag{5}$$

where $i = \sqrt{-1}$, $\omega$ is the angular frequency and $\sigma'$ a proportionality factor. The particular case of a Warburg type impendance implies that $\alpha = 0.5$.[13] In general, $\alpha$ is related to a kind of surface like topography and $\sigma'$ to a function of the electrolyte resistivity and double layer capacitance.[14,15] On this basis, equation 5 refers to a coupling of dissipative and energy storing processes. The simulated impendance diagrams for $FeS_2$/KI and KBr 0.5 M at 25 °C are illustrated in Figure 9. Although the fit is not exactly at intermediate frequencies to that of the experimental points, nevertheless the trace of the simulated curve approaches the experimental one. This result strongly support our assumption of the presence of at least three relaxation times at the pyrite/electrolyte interface. The values of the parameters obatained by fitting the set of experimental curves at different temperatures, *e. g.*, $C_{sc}$, and $R_{ct}$, and $\alpha$ are displayed in the Figure 10. Several important conclusions can be dedu-

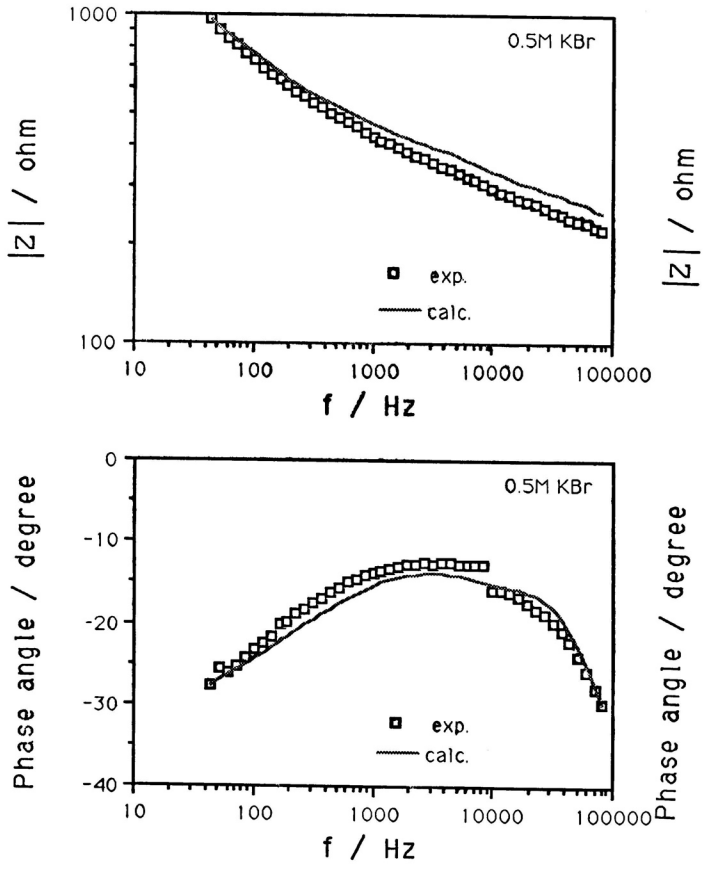


Figure 9. *Fig. 9 to ba continued*

ced from these results. As it was expected, from the system $FeS_2$/KI the capacity of the space charge region, $C_{sc}$, remains independent of the temperature (Figure 10 a), which supports the idea that the effect of the temperature on the charge transfer is only an activation process and not due to a displacement of the semiconductor bands. In the case of the $FeS_2$/KBr system, the contribution of the corrosion process, at temperature higher than 35 °C, is enhanced even if the concentration of the reducing species is doubled. Tentatively this would mean that an oxide layer is acting as a capacitive element in series with the semiconductor space charge capacity. This modification of the pyrite surface in this medium enhanced with the temperature is supported by the recording of the cyclic voltammetric curve, see Figure 1D, and the change of slope in the temperature varying photopotential. The values obtained for the parameter $\alpha$ vary around 0.5 (Figure 10 b). This value was directly calculated from the experimental points on the impendance plane plot: $\alpha = 2$ arc tg $(\psi)/\pi$ (typical frequency range 44 to 300 Hz). This parameter is $>0.5$ and increases almost linearly with the temperature in the case of $FeS_2$/KI in the dark; remaining constant and $<0.5$ for the $FeS_2$/KBr system. The fact

*Fig. 9 continued*

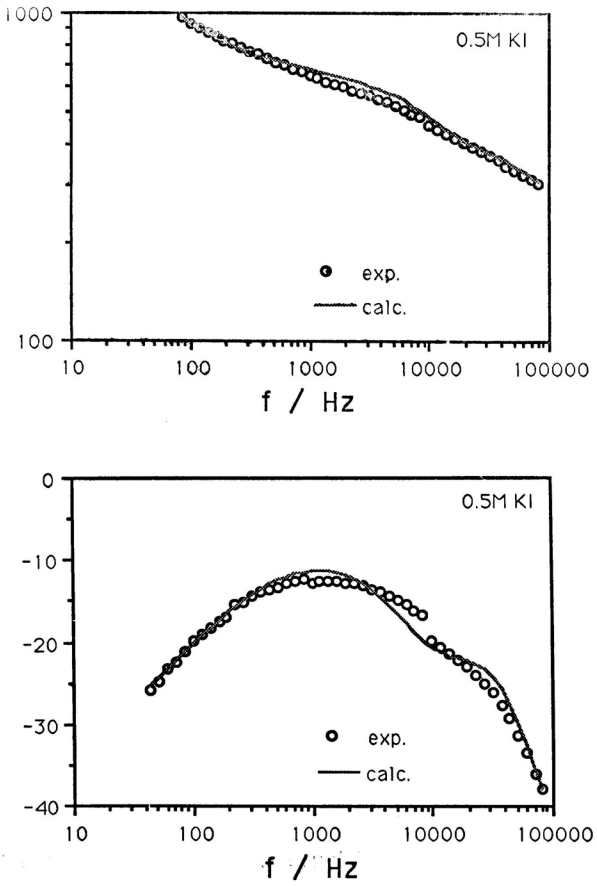


Figure 9. Comparison between measured and calculated Bode plots (impendance magnitude and phase angle) of the systems containing 0.5 M KI and 0.5 M KBr in darkness at 25 °C.

that for the system $FeS_2$/KI this effect is reversible, when decreasing the temerature, this would mean that this parameter does not actually point towards an increase of the roughness of the surface but probably to a certain dynamic of the interface induced by the active coordination sites. This dynamic is clearly observed when illuminating this interface, since this line is simply shifted parallel towards lower values (curve not shown in the Figure 10 b) increasing again towards higher temperatures. From the inverse charge transfer resistance as a function of the inverse of temperature, Figure 10 c, the activation energy for systems containing KI and KBr are: 0.30 and 0.36 eV, respectively.

## CONCLUSION

Results obtained by temperature variation and by the impedance measurements lead to the conclusion that chemical interaction between electron do-

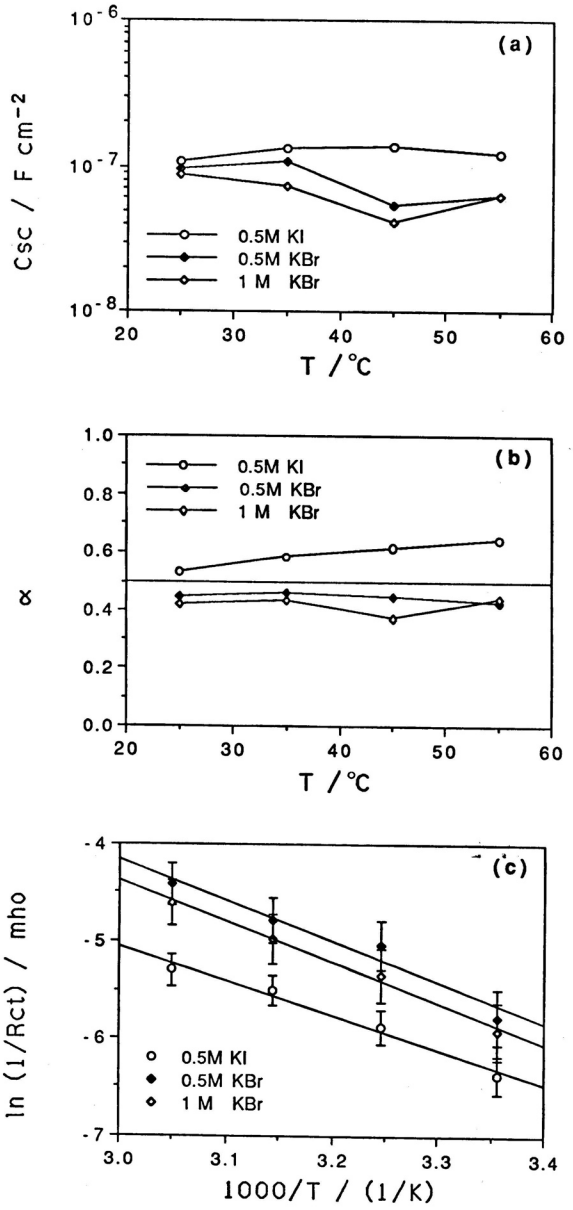


Figure 10. For the systems containing 0.5 M KI (at —0.24 V/$Hg_2SO_4$), 0.5 M KBr and 1 M KBr (at 0.28 V/$Hg_2SO_4$). (a) depicts the deduced $C_{sc}$ as function of temperature, (b) the fitting parameter a as a function of temperature and (c) the Arrhenius plot for the charge transfer conductance.

nating species and the pyrite electrode surface, as observed with $I^-$, $Br^-$, $[Fe(CN)_6]^{4-}$ and Mohr' salt, is supporting electron transfer and reducing electrode corrosion. An interfacial coordination chemistry has to be involved with iron d-states.

## REFERENCES


1. J. C. Bailar, H. J. Emeléus, R. Nyholm, and A. F. Trotman-Dickenson, *Comprehensive Inorganic Chemistry*, Vol. 2 p. 796, Permagom Press, London, 1973.
2. A. Ennaoui, S. Fiechter, and H. Tributsch, *J. Electrochem. Soc.* **132** (1985) 1579.
3. B. E. Conway, J. C. H. Ku, and F. C. Ho, *J. Colloid Interface Sci.* **75** (1980) 357.
4. K. K. Mishra and K. Osseo-Asare, *J. Electrochem. Soc.* **135** (1988) 1898; *idem* **135** (1988) 2502.
5. J. Luck, A. Hartmann, and S. Fiechter, *Fresenius Z. Anal. Chem.* **334** (1989) 441.
6. A. Ennaoui and H. Tributsch, *J. Electroanal. Chem.* **204** (1986) 185.
7. X.-P. Li, N. Alonso Vante, and H. Tributsch, *J. Electroanal. Chem.* **242** (1988) 255.
8. S. Fiechter, J. Mai, A. Ennaoui, and W. Szacki, *J. Crystal Growth* **78** (1986) 438.
9. N. Alonso Vante, G. Chatzitheodorou, S. Fiechter, N. Mgoduka, I. Poulios, and H. Tributsch, *Solar Energy Mat.* **18** (1988) 9.
10. A. Ennaoui, S. Fiechter, W. Jaegermann, and H. Tributsch, *J. Electrochem. Soc.* **133** (1986) 97.
11. A. N. Buckley and R. Woods, *Appl. Surface Sci.* **27** (1987) 437.
12. L. C. Schumacher and M. J. Dignam, *J. Electrochem. Soc.* **136** (1989) 3396.
13. J. Ross Macdonald (Ed.), *Impedance Spectroscopy*, Wiley & Sons. New York (1987).
14. W. Scheider, *J. Phys. Chem.* **79** (1975) 127.
15. L. Nykos and T. Pajkossy, *Electrochim. Acta* **30** (1985) 1533.


## SAŽETAK

### Piritna anoda/redoks elektrolit granica faza: karakterizacija interakcije reducirajuće vrste s piritom mjerenjem temperaturne ovisnosti

*N. Alonso-Vante i H. Tributsch*

Opisana su mjerenja temperaturne ovisnosti interakcije piritne fotoanode s redoks elektrolitima. Kao elektrolit upotrebljeni su oni s anionima $I^-$, $Br^-$, $Fe(CN)_6^{-4}$, i kationom $Fe^{3+}$ u sulfatnom mediju. Proučavane su ovisnosti struja — potencijal i mjerena međufazna impedancija u tami i uz osvjetljavanje bijelom svjetlošću iz halogen/volframskog izvora. Energija aktivacije za KI i KBr dobivena mjerenjima kinetičkih parametara je 0,26 i 0,46 eV. Za iste elektrolite, vrijednosti dobivene iz temperaturne ovisnosti otpora prijenosa naboja su 0,30 i 0,36 eV, što se smatra dobrim slaganjem.